Hidden symmetries enhance quantum transport in Light Harvesting systems

Tobias Zech,[1] Roberto Mulet,[2] Thomas Wellens,[1] and Andreas Buchleitner[1]

[1] *Physikalisches Institut, Albert-Ludwigs-Universitat Freiburg, Hermann-Herder-Str. 3, D-79104 Freiburg, Germany*

[2] *Complex System Group, Department of Theoretical Physics, University of Havana, Cuba and Physikalisches Institut, Albert-Ludwigs-Universitat Freiburg, Hermann-Herder-Str. 3, D-79104 Freiburg, Germany**

(Dated: March 4, 2013)

For more than 50 years we have known that photosynthetic systems harvest solar energy with almost unit *quantum efficiency*. However, recent experimental evidence of *quantum coherence* during the excitonic energy transport in photosynthetic organisms challenges our understanding of this fundamental biological function. Currently, and despite numerous efforts, the causal connection between coherence and efficiency is still a matter of debate. We show, through the study of extensive simulations of quantum coherent transport on networks, that three dimensional structures characterized by centro-symmetric Hamiltonians are statistically more efficient than random arrangements. Moreover, we demonstrate that the experimental data available for the electronic Hamiltonians of the Fenna-Mathew-Olson (FMO) complex of sulfur bacteria and of the crypophyte PC645 complex of marine algae are consistent with this strong correlation of centro-symmetry with quantum efficiency. These results show that what appears to be geometrically disordered complexes may well exhibit a hidden symmetry which enhances the energy transport between chromophores. We are confident that our results will motivate research to explore the properties of nearly centro-symmetric Hamiltonians in more realistic environments, and to unveil the role of symmetries for quantum effects in biology. The unravelling of such symmetries may open novel perspectives and suggest new design principles in the development of artificial devices.

arXiv:1205.5519v1 [physics.bio-ph] 23 May 2012

I. INTRODUCTION

The apparatus used by photosynthetic organisms to harvest the sun's energy is both complex and highly efficient. Although it appears differently in different species, some features always persist: Photons are absorbed by pigments, usually chlorophyll or carotenoid molecules, and transmitted to a reaction center *(RC)*, where the primary chemical reactions of photosynthesis occur [1]. Photosynthetic structures contain far more chlorophyll molecules than *RC*s, and the former constitute molecular networks which pass the energy of an absorbed photon to the *RC*, where it is trapped [1–3].

In recent years, ultrafast optics and nonlinear spectroscopy experiments provided new insight into excitonic energy transport in photosynthetic organisms [5–7]. These experiments report the existence of long coherence times, suggesting that *quantum coherence* may play a fundamental role in the highly efficient transport of excitations, and trigger renewed theoretical interest.

A well established strategy to simulate the quantum excitation transport in such molecular complexes is the dynamical propagation of the electronic Hamiltonian in the presence of the many degrees of freedom of the environment [8–15]. This line of thought may suggest that proper tuning of the interaction between system and environment is responsible for the long coherence times and the efficient transport [16]. However, the computationally obtained coherence times ($t_c \sim 250$ fs) [15] are smaller than the experimentally reported ($t_c \sim 660$ fs) [5]. Moreover, the complexity of the quantum dynamics grows exponentially with the number of strongly coupled degrees of freedom [15], rendering approximations unavoidable, even in a full-fledged computational approach. Since, in addition, also the available experimental data characterizing the complexes have large uncertainties, most computational methods use effective descriptions. This contrasts with the fact that the non-trivial, system-specific information on complex quantum systems is inscribed into the fluctuations of characteristic observables, rather than in their average behavior [17–20].

On the other hand, simplified models [22–24] that mimic the dynamics by those of two coupled two level systems interacting with the environment, may help to identify some minimal ingredients that must be included into a general theory. However, because of their simplicity, they disregard many of the structural features of the light harvesting complexes – possibly those that are most relevant for the transport efficiency in realistic systems.

Therefore, in our present contribution, we attempt to incorporate most of the documented properties of the underlying electronic Hamiltonians, and yet to outline a model as simple as possible. We will see that 3D random networks are very likely to perform efficiently whenever their Hamiltonians exhibit centro-symmetry. On this basis, we will provide strong evidence that the transport efficiencies across light harvesting complexes indeed substantially depend on the structural properties of the apparently disordered macromolecular Hamiltoni-

*Electronic address: roberto.mulet@gmail.com; Electronic address: mulet@fisica.uh.cu

ans. In particular, we will show that, specifically for the reported Hamiltonians of the FMO8 and PC645 pigment complexes, centro-symmetry defines an evolutionary advantage.

II. THE MODEL

Inspired by the structure of the FMO network – seven (FMO7) [25, 26] or eight (FMO8) [27] chromophores that are connected through dipolar interactions – we study the simplest possible random model which can grasp its essential ingredients: A small random network with N sites, where the coherent transport of a single excitation is generated by the Hamiltonian

$$H = \sum_{i\neq j=1}^{N} V_{i,j}\ \sigma_+^{(j)}\sigma_-^{(i)}\,. \tag{1}$$

Here, $\sigma_+^{(j)}$ and $\sigma_-^{(i)}$ mediate excitations and de-excitations of sites j and i, from the local electronic ground state to the local excited state, and vice versa. The excitation transfer $\sigma_+^{(j)}\sigma_-^{(i)}$ from site i to site j has a strength $V_{i,j} = V_{j,i} = \alpha/r_{i,j}^3$, consistent with an isotropic dipolar interaction, with $r_{i,j} = |\vec{r}_i - \vec{r}_j|$, and the $\vec{r}_j$ the position vectors of individual sites. Input and output sites define the pole of a sphere of diameter d. The positions of the remaining molecular sites are randomly chosen within this sphere, what induces a random distribution of the remaining $V_{i,j}$. Networks for which one of the distances $r_{i,j}$ was smaller than $d/100$ were discarded in the analysis, in order to avoid singular coupling strengths [21]. The excitation initially is injected at the input site $|\text{in}\rangle = |1\rangle$, from where it is to be transferred to the output site $|\text{out}\rangle = |N\rangle$. The coupling constant $V_{1,N} = \alpha/d^3$ between these two sites sets the natural time-scale of the dynamics induced by H. The intuition is that the additional sites, if properly placed, can mediate a multitude of transition amplitudes from input to output, which interfere *constructively* upon transmission, and thus ease the excitation transfer. A network will be considered *efficient* if the initial excitation is transferred to the output site in a time significantly smaller than the Rabi coupling time $T = \pi/2|V_{1,N}|$ between $|\text{in}\rangle$ and $|\text{out}\rangle$, with high probability. For a quantitative assessment, we define the figure of merit [28, 29]

$$\mathcal{P} = \max_{t\in[0,\mathcal{T}]} |\langle N|e^{-iHt}|1\rangle|^2\,, \text{ with } \mathcal{T} = 0.1\times\pi/2|V_{1,2}|\,. \tag{2}$$

Indeed, we showed earlier that $\mathcal{P}$ fluctuates strongly with different realizations of the random molecular network, and reaches large values close to unity with finite probability. However, while it is therefore natural to ask for necessary and/or sufficient conditions on the networks's structure such as to guarantee large values of $\mathcal{P}$, no *design principles* were so far identified. This is the purpose of our present contribution.

III. RESULTS

While near-optimal random networks – in the sense of giving rise to large values of $\mathcal{P} \simeq 1$ – do not exhibit apparent symmetries in their 3D geometry, it was observed that the individual sites' populations indeed do display a near-symmetric structure on the time axis, under exchange of input and output site, as well as of properly defined pairs of intermediate sites (see Fig. 2 in [29]). This must be inherited from an exchange symmetry of pairs of two-site coupling matrix elements of the underlying Hamiltonian, and evokes an analogy with $N\times N$ *centro-symmetric* matrices, which are defined by $H_{i,j} = H_{N-i+1,N-j+1}$, i.e., $JH = HJ$, where J is the exchange matrix, $J_{i,j} = \delta_{i,N-j+1}$, that exchanges site 1 with site N, 2 with $N-1$, etc. This type of Hamiltonians is known to be tunable towards optimal excitation transfer [30–32]. We now quantify the transfer efficiency (2) of a given Hamiltonian, and correlate this with the Hamiltonian's centro-symmetry, measured by $\epsilon = \min_S ||H - J^{-1}HJ||$, where $||\dots||$ denotes the Hilbert-Schmidt norm, i.e., $||A|| = \sqrt{\text{Tr}A^\dagger A}$ [33]. The quantity ϵ measures the root-mean square deviation of a network Hamiltonian from its image under J, minimized over all possible permutations S of the intermediate sites $2,\dots,N-1$. Figure 1 shows the correlation plot on a triple logarithmic scale, for $N = 7$, and sampling 10^8 independent random realizations of the network.

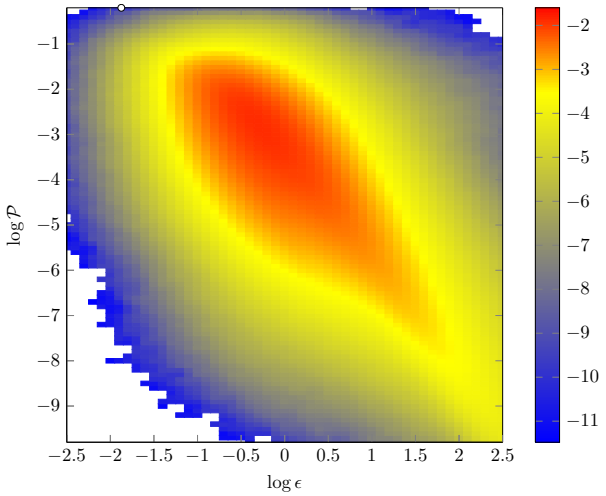

FIG. 1: Correlation between efficiency $\mathcal{P}$ and centro-symmetry ϵ of 10^8 randomly generated 3D networks composed of seven sites. The color code indicates the logarithm of the probability density of a pair $(\log(\epsilon), \log(\mathcal{P}))$. The white circle close to the top left corner represents a quasi optimal configuration found by a genetic algorithm.

A very strong and, given the variance of $\mathcal{P}$ and ϵ over several orders of magnitude, unambiguous correlation between centro-symmetry (small values of ϵ) and transfer efficiencies is evident. So is the rather low probability to generate a high efficiency molecular conforma-

tion by random sampling. On the other hand, the observed strong statistical correlation implies that an iterative search for highly efficient networks in conformation space will with very high probability move towards higher degrees of centro-symmetry, and hence acts as an evolutionary *funnel*. This is confirmed by a genetic algorithm [34] that optimizes the structure of the networks to achive maximum efficiency: Starting from random networks, located with high probability close to the global maximum of the distribution in Figure 1, i.e. approx. at $\log(\epsilon) \simeq -0.5$, $\log(\mathcal{P}) \simeq -3$, the algorithm generates configurations with almost unit efficiency and very low centrosymmetry. An exemplary output configuration is indicated by the white circle in Figure 1: While the deviation from the centro-symmetry is reduced by approximately 1.5 orders of magnitude, the network's efficiency increases by about 3 orders of magnitude.

That the observed correlation between $\mathcal{P}$ and ϵ is in itself of quantum origin is suggested by our initially formulated intuition on the role of the intermediate sites which mediate the excitation transfer from $|\text{in}\rangle$ to $|\text{out}\rangle$. This is underpinned by inspection of the analogously generated correlation plots in Figure 2, though in the presence of environment-induced dephasing locally at each individual molecular site. The excitation transfer dynamics is then no longer described by the unitary evolution alone, but rather by a Lindblad equation $\dot{\varrho}(t) = -\mathrm{i}\,[H, \varrho(t)] + L_{\text{deph}}(\varrho(t))$, with the Lindblad term

$$L_{\text{deph}}(\rho) = -4\gamma \sum_{i \neq j = 1}^{7} |i\rangle\langle i|\varrho|j\rangle\langle j|\,, \qquad (3)$$

and $|\text{i}\rangle$ and $|\text{j}\rangle$ the N-site electronic state where the excitation is located at the i^{th}, respectively j^{th} site. As the dephasing rate γ is tuned from zero over one and ten to hundred incoherent events per Rabi coupling time T, the distribution in the correlation plot essentially rotates from a strongly increasing efficiency with increasing centro-symmetry to an essentially centro-symmetry-independent distribution, at the largest dephasing rates. However, note that the correlation prevails even for relatively large dephasing rates of $\gamma = 10T^{-1}$, what corresponds to one incoherent event within the time interval that we chose to define $\mathcal{P}$ in (2).

We now need to validate the relevance of our above findings for the actual design of light harvesting complexes as they abound in nature. Clearly, the strong correlation between transfer efficiency and centro-symmetry of the network as evident from Figs. 1 and 2 was deduced from unrestricted, uniform statistical sampling over a random Hamiltonian of the form (1). However, actual biological functional units are sufficiently well characterized (by spectroscopic means) to locate them in a comparably small sub-volume of conformation space. Therefore, we now focus on the trade-off between centrosymmetry and transfer efficiency using published data of the FMO8 protein [35] and the PC645 [36] light harvesting complexes (of sulfur bacteria and marine algae,

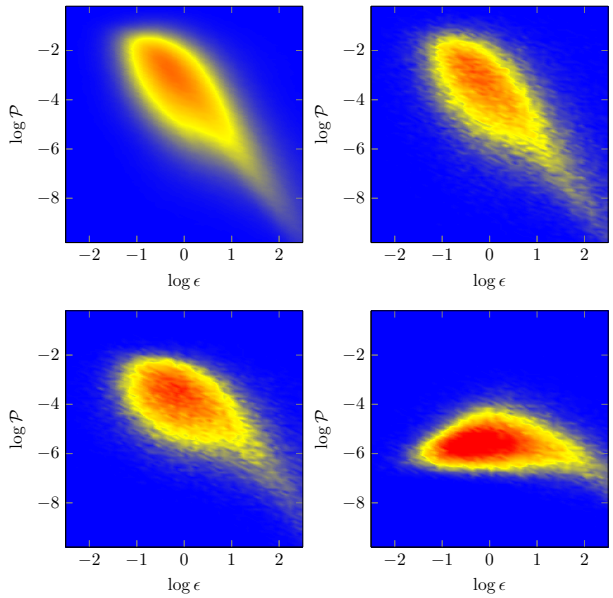

FIG. 2: Histogram for the open system dynamics of mirrorsymmetry ϵ vs. transport efficiency $\mathcal{P}$, for different values of the dephasing rate in the site basis, $\gamma =$ (upper left) 0, (right) 1, (lower left) 10, (right) 100, in units of the characteristic time scale $T = \pi/2|V_{\text{in,out}}|$. The color code indicates the probability density of a pair $(\log(\epsilon), \log(\mathcal{P}))$. The histograms are generated from 10^5 random networks for $\gamma > 0$, and 10^8 for $\gamma = 0$ (as in Figure 1, but on linear scale). The correlation between transfer efficiency and centrosymmetry is less pronounced for larger values of γ.

respectively) as our point of departure. Both these complexes are represented by a network of eight dipole-coupled two-level systems, and thus comply with our abstract model from above.

In order to define an unbiased benchmark in comparison to which we can quantitatively assess the centrosymmetry properties of the actual FMO8 and the PC645 Hamiltonian, we use an ensemble of random Hamiltonian matrices constructed as follows: the off-diagonal elements of these random Hamiltonians are modeled as identically and independently distributed random variables, which are all chosen from the same Gaussian distribution. The mean value and standard deviation of this distribution is extracted as the mean and as the standard deviation of the non-diagonal elements of the published data for the FMO8 and PC645 complex, respectively (see the complementary material in Sec. VI B). In order to avoid centrosymmetry to be masked by the biological complexes' on-site energies induced by their coupling to (environmental) background degrees of freedom, we in addition set all diagonal matrix elements equal to their average value.

The distribution of the centro-symmetry ϵ with respect to the input and output sites thus obtained is represented by the green histograms, for FMO8 and PC645, respectively, in Figure 3, and defines our unbiased benchmark distribution. For the FMO8, the input site is the site recently added to the structure of the protein, and the

output site is usually named "site 3" in the biological literature [35]. For the PC645, we identify the DBVc and PCBd82 molecules with the input and output sites, respectively [36].

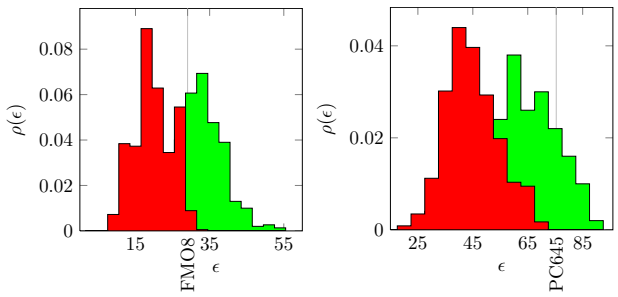

FIG. 3: Green: Centro-symmetry distributions for Gaussian random ensembles with mean and standard deviation extracted from the original FMO8 (left) and PC645 (right) structure data [35, 36]. Red: Centro-symmetry distributions for efficient systems obtained by evolutionary optimization of the FMO8 and PC645 Hamiltonians. The vertical lines indicate the centro-symmetry of the original FMO8 and PC645 Hamiltonians, respectively.

The vertical lines in Fig. 3 indicate the centro-symmetries of the effective FMO8 and PC645 Hamiltonians, respectively, extracted from the published data. Since, in both cases, the complexes' centro-symmetries are located in the bulk of the unbiased distribution, they do not exhibit any significant symmetry properties. This is consistent with the time evolution of the single site populations as presented in Figure 4, which clearly show very unsatisfactory coherent transfer efficiency, for both molecular networks. Indeed, as we have checked, *all* elements of the random ensemble display similarly mediocre efficiencies.

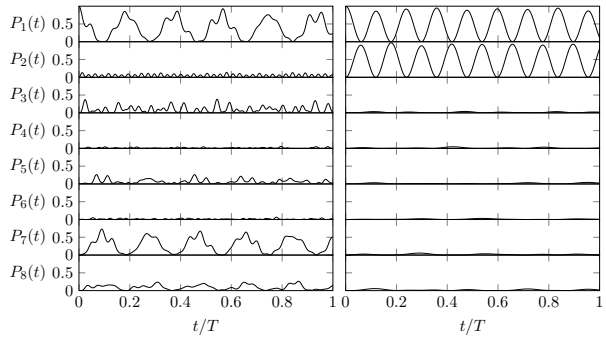

FIG. 4: Single site populations of the FMO8 (left) and PC645 (right) light harvesting complexes, with inter-site coupling matrix elements extracted from published structure data [35, 36], and on-site energies replaced by their mean. Initially, the excitation is located at site 1. Clearly, the transfer efficiency towards site 8 is mediocre, for FMO8 as well as for PC645. Site labels 1 and 8 correspond to sites 1 and 3 for FMO8 [35], and to DBVc and PCBd81 for PC645 [36], respectively.

We now assess how close FMO8 and PC645 structures are, in conformation space, to more centro-symmetric conformations, with higher transfer efficiencies. For this purpose, we generate a new ensemble of network Hamiltonians, by repeated execution of N=10000 iterations of a simple genetic algorithm (see Sec. VI A), seeded by the published network Hamilonians [35, 36] as indicated by the vertical lines in Figure 3. This results in the red histograms in Figure 3, which are clearly shifted towards higher centro-symmetries (i.e., smaller values of ϵ), by more than the original benchmark distributions' widths. We verified that all the thus optimized Hamiltonians mediate essentially perfect excitation transfer. Moreover, even the *average* Hamiltonian obtained from an equally weighted sum of the optimized ensemble does so! This is clearly demonstrated by Figure 5, where the time dependence of the individual site populations is monitored, as generated by this average Hamiltonian. Since different,

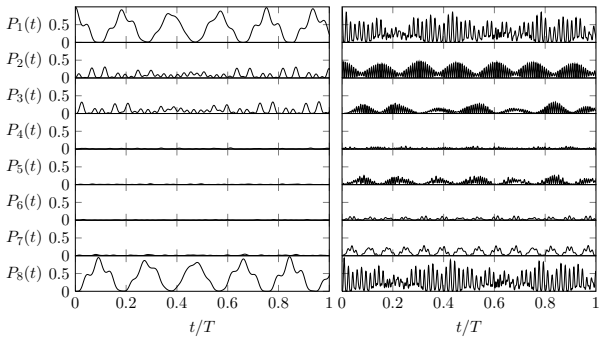

FIG. 5: Single-site populations for genetically optimized FMO8 (left) and PC645 (right) light harvesting complexes, with inter-site coupling matrix elements given by an equally weighted average over 10^3 optimized Hamiltonians generated by the genetic algorithm. Site labeling as in Fig. 4. Essentially optimal transfer efficiencies are achieved in both cases.

individually optimized Hamiltonians generally do not commute, this is a highly nontrivial result which underpins, in particular, that evolutionary optimization seeded by the FMO8 and PC645 structures converges into essentially optimal transfer efficiencies, in a statistically robust sense. Furthermore, this observation highlights close connection between centro-symmetry and efficiency, since a sum of centro-symmetric Hamiltonians remains centro-symmetric. Finally, inspection of the thus obtained average optimal Hamiltonian's matrix elements shows that most of them can be obtained by weak perturbation of those as inferred spectroscopically (see Sec. VI B).

In contrast to the above results when starting out from the FMO8 and PC645 structures, the very same genetic optimization leaves the distributions as indicated by the green histograms in Figure 3 essentially unaffected, with correspondingly bad transfer efficiencies, when seeded by any of the elements of our random benchmark ensemble. This markedly distinct behavior of the genetic optimization for FMO8 and PC645 on the one hand, and of random benchmark Hamiltonians on the other there-

fore strongly suggests centro-symmetry as a hidden design principle.

IV. CONCLUSIONS

Symmetry is a key concept in physics, relevant in fields as diverse as High Energy Physics and Condense Matter. In our present work, we provide strong evidence to support the hypothesis that hidden symmetries in the Hamiltonian of apparently disordered biological structures foster quantum capabilities. In particular, we have shown that in random artificial networks, but also in the biologically relevant light harvesting complexes FMO8 and PC645, (nearly) centro-symmetric Hamiltonians define a robust design principle to mediate coherence-induced, efficient quantum transport. Note that this hidden symmetry property could only be extracted by a statistical analysis of suitably constructed matrix ensembles, gauged against experimentally inferred average data. This is not surprising, since complex quantum systems typically exhibit very intricate spectral properties, with in general only small embedded regions (e.g. on the energy axis or with respect to some control parameter(s)) of locally well-defined quantum numbers. In contrast to the global symmetries of integrable quantum systems, the associated (local) symmetries of complex systems are typically not given by explicitly defined integrals of motion, and this is why they are hard to detect – and yet may manifest a dramatic and robust impact on the systems' dynamical properties. We trust that our findings may define a good starting point for the design of new devices for efficient energy transduction [37], and are confident that the here unveiled conspiracy of symmetry and quantum coherence in an apparently disordered system may be instrumental in other biological systems [38].

V. ACKNOWLEDGMENTS

We are indebted to Irene Burghardt, Rienk van Grondelle, Shaul Mukamel, Torsten Scholak, Greg Scholes and Mattia Walschaers for stimulating discussions and useful insights. R.M. acknowldeges support by the Alexander von Humboldt Foundation through a research fellowship.

VI. SUPPLEMENTARY MATERIAL

A. Genetic Algorithm

To iteratively optimize the transfer efficiency we proceed as follows:

Step 1: Read the original Hamiltonian: H^*.

Step 2: Starting from H^*, generate M configurations by randomly perturbing all matrix elements H_{ij} of H^*, according to a Gaussian distribution with standard deviation σ, initially set to $\sigma_0 = H_{ij}/10$.

Step 3: From these configurations (including H^*), choose the one with the largest efficiency. This configuration defines the new H^*.

Step 4: Repeat steps 2-4 until the maximum number N of iterations is reached. At the nth iteration, perturb the matrix element H_{ij} by a Gaussian distribution with standard deviation $\sigma_n = \sigma_0/n$.

In our optimization of the FMO8 and PC645 structures, $M = 100$ and $N = 10000$ always achieve convergence. Note that the algorithm only optimizes with respect to the transfer efficiency, and not with respect to the centrosymmetry.

B. Hamiltonians

A comparison of the off-diagonal elements of the average optimized Hamiltonian with the original FMO8 and PC645 Hamiltonians as given in the literature is shown in Figs. 6 and 7. Using the standard notation from the literature, the rows in the Hamiltonian of Fig. 6 (FMO8) correspond to the sites with labels 8, 1, 2, 4, 5, 6, 7, and 3. Likewise, the rows in the Hamiltonian of Fig. 7 (PC645) correspond to sites labeled by DBVc, PCBc82, DBVd, MBVa, MBVb, PCBc158, PCBd158, and PCBd82. Mean values $\overline{V}$ and standard deviations ΔV which define the random ensembles represented by the green histograms in Fig. 3 are derived from the data in Figs. 6, 7 as: $\overline{V} = 2.6$, $\Delta V = 34.5$ (FMO8), and $\overline{V} = 21.3$, $\Delta V = 67.0$ (PC645), respectively.

[1] D. Voet and P. Voet, *Biochemistry*, John Wiley & Sons (2000) (3rd edition)

$$\begin{pmatrix} \dots & -12.7/-11.1 & 35.9/39.5 & 3.6/7.9 & -1.6/-1.6 & 4.8/4.4 & -7.0/-9.1 & 1.4/1.4 \\ \dots & \dots & -12.8/-12.2 & 6.4/5.7 & -96.4/-62.3 & -4.9/-4.6 & 21.9/35.1 & 3.8/3.4 \\ \dots & \dots & \dots & -96.2/-98.0 & -6.0/-5.9 & 7.9/7.1 & -12.4/-15.1 & 2.8/5.5 \\ \dots & \dots & \dots & \dots & 7.9/7.6 & 1.5/1.6 & 12.7/13.1 & 35.8/29.8 \\ \dots & \dots & \dots & \dots & \dots & -40.9/-64.0 & -16.2/-17.4 & -9.3/-58.9 \\ \dots & \dots & \dots & \dots & \dots & \dots & 134.9/89.5 & -1.2/-1.2 \\ \dots & \dots & \dots & \dots & \dots & \dots & \dots & -7.9/-9.3 \\ \dots & \dots & \dots & \dots & \dots & \dots & \dots & \dots \end{pmatrix}$$

FIG. 6: Off-diagonal elements of the average Hamiltonian after optimizing the FMO8 structure with a genetic algorithm (left), and of the original, spectroscopically inferred FMO8 Hamiltonian (right) [35].

$$\begin{pmatrix} \dots & -10.6/-46.8 & 106.4/319.4 & -5.7/-9.6 & -23.8/-43.9 & 18.4/20.3 & 3.2/25.3 & -0.7/-20.0 \\ \dots & \dots & 14.4/21.5 & -17.1/-15.8 & 56.1/53.8 & 10.9/11.0 & 29.2/29.0 & 5.1/48.0 \\ \dots & \dots & \dots & 30.2/43.9 & 7.1/7.7 & 16.3/30.5 & 23.3/29.0 & 105.4/48.0 \\ \dots & \dots & \dots & \dots & 4.5/4.3 & -154.4/-86.7 & -3.0/-2.9 & 14.5/49.3 \\ \dots & \dots & \dots & \dots & \dots & 3.5/3.4 & 108.4/86.2 & -20.2/-14.7 \\ \dots & \dots & \dots & \dots & \dots & \dots & 7.9/7.8 & 11.4/10.0 \\ \dots & \dots & \dots & \dots & \dots & \dots & \dots & -7.6/-10.7 \\ \dots & \dots & \dots & \dots & \dots & \dots & \dots & \dots \end{pmatrix}$$

FIG. 7: Off-diagonal elements of the average Hamiltonian after optimizing the PC645 structure with a genetic algorithm (left), and of the original, spectroscopically inferred PC645 Hamiltonian (right) [36].

[2] X. Hu and K. Schulten, How Nature Harvests Sunlight , Physics Today, **August**, 28-33 (1997)

[3] G. R. Fleming and R. van Grondelle, The Primary Steps of Photosynthesis, Physics Today, **February**, 48-55 (1994)

[4] H. Lee, Y.C. Cheng and G. Fleming, Coherence Dynamics in Photosynthesis: Protein Protection of Excitonic Coherence, Science **316**, 1462-1465 (2007)

[5] G. Engel, T. R. Calhoun, E.L. Read, Taek-Kyu Ahn, T. Mancal, Y.C. Cheng, R. E. Blankenship and G. Fleming, Evidence for wavelike energy transfer through quantum coherence in photosynthetic complexes, Nature **446**, 782-786 (2007)

[6] E. Collini, C. Y. Wong, K. E. Wilk, P. M. G. Curmi, P. Brumer and G. D. Scholes, Coherently wired light-harvesting in photosynthetic marine algae at ambient temperature, Nature **463**, 644-647 (2010)

[7] D.B. Turner, R. Dinshaw, Kyung-K. Lee, M. S. Belsley, K. E. Wilk, P. M. G. Curmi and G. D. Scholes, Quantitative investigations of quantum coherence for a light-harvesting protein at conditions simulating photosynthesis, Chem. Phys. Chem. **14**, 4857-4874 (2012)

[8] A. Ishizaki and G. R. Fleming, Theoretical examination of quantum coherence in a photosynthetic system at physiological temperature, PNAS **106**, 17255-17260 (2009)

[9] M. Mohseni, P. Rebentrost, S. Lloyd and A. Aspuru-Guzik, Environment-assisted quantum walks in photosynthetic energy transfer, J. Chem. Phys. **129**, 174106 (2008)

[10] M. B. Plenio and S. F. Huelga, Dephasing-assisted transport: quantum networks and biomolecules, New J. Phys. **10**, 113019 (2008)

[11] A. Olaya-Castro , C-F Lee, F. Fassioli-Olsen and N.F. Johnson, Efficiency of excitation transfer in photosynthesis under quantum coherence, Phys. Rev. B **78**, 085115 (2008)

[12] P. Nalbach, A. Ishizaki, G. R. Fleming and M. Thorwart, Iterative path-integral algorithm versus cumulant time-nonlocal master equation approach for dissipative biomolecular exciton transport. New J. of Phys. **13**, 063040-063053 (2011)

[13] A. Pereverzev, E. R. Bittner, and I. Burghardt, Energy and charge-transfer dynamics using projected modes, J. Chem. Phys. **131**, 034104 (2009)

[14] A. Shabani, M. Mohseni, H. Rabitz and S. Lloyd, Efficient estimation of energy transfer efficiency in light-harvesting complexes. arxiv. 1103.3823

[15] P. Nalbach, D. Braun and M. Thorwart, Exciton dynamics and quantumness of energy transfer in the Fenna-Mathews-Olson complex. Phys. Rev. E **84**, 041926 (2011)

[16] S. Lloyd, M. Mohseni, A. Shabani and H. Rabitz, The quantum Goldilocks effect: on the convergence of timescales in quantum transport, arXiv:1111.4982

[17] M.C. Gutzwiller, The Semi-Classical Quantization of Chaotic Hamiltonian Systems, in *Chaos and Quantum Physics*, ed. by M.-J. Giannoni, A. Voros and J. Zinn-Justin, Les Houches, Session LII, 1989, Elsevier Science Publishers B.V., 1991, pp. 201-249

[18] S. S. Skourtis, D. H. Waldeck and D. N. Beratan, Fluctuations in biological and bioinspired electron-transfer reactions, Annu. Rev. Phys. Chem. **61** 461-485 (2010)

[19] R. Alicki and W. Miklaszewski, A resonance mechanism of efficient energy transfer mediated by Fenna-Matthews-Olson complex, J. Chem. Phys. **136**, 134103 (2012)

[20] T. Scholak, F. Mintert, T. Wellens, and A. Buchleitner, Semicond. Semimet. **83**, 1 (2010)

[21] T. Scholak, *Transport and coherence in disordered networks*, Dissertation, Albert-Ludwigs-Universität Freiburg (2011), http://www.quantum.uni-freiburg.de

[22] J. B. Gilmore and R. H. McKenzie, Spin boson models for quantum decoherence of electronic excitations of biomolecules and quantum dots in a solvent, J. Phys.: Condens. Matter **17**, 1735 (2005)

[23] L. A. Pachón and P. Brumer, The physical basis for long-lived electronic coherence in photosynthetic light harvesting systems, J. Phys. Chem. Lett. **2**, 2728 (2011)

[24] O. Mülken and T. Schmidt, Environment-assisted quantum transport and trapping in dimers, Phys. Rev. E **82**, 042104 (2010)

[25] R. E. Fenna, B. W. Matthews,Chlorophyll arrangement in a bacteriochlorophyll protein from Chlorobium limicola, Nature **258**, 573-577 (1975)

[26] D. E. Tronrud, M. F. Schmid and B. W. Mathews, Structure and X-ray amino acid sequence of a bacteriochlorophyll a protein from prosthecochloris aestuarii refined at 1.9 Å resolution, J. Mol. Biol. **188**, 444-454 (1986)

[27] D.E. Tronrud, J. Z. Wen, L. Gay and R.E. Blankenship, The Structural Basis for the Difference in Absorbance Spectra for the FMO Antenna Protein from Various Green Sulfur Bacteria, Photosynth. Res. **100** 79-87 (2009)

[28] T. Scholak, T. Wellens and A. Buchleitner, The optimization topography of exciton transport, Europhys. Lett. **96**, 10001 (2011)

[29] T. Scholak, F. de Melo, T. Wellens, F. Mintert, and A. Buchleitner, Efficient and coherent excitation transfer across disordered molecular networks, Phys. Rev. E **83**, 021912 (2011)

[30] A. Cantoni and P. Butler, Eigenvalues and eigenvectors of symmetric centrosymmetric matrices, Linear Alg. Appl. **13**, 275 (1976)

[31] C. Albanese, M. Christandl, N. Datta and A. Ekert, Mirror Inversion of Quantum States in Linear Registers, Phys. Rev. Lett. **93**, 230502 (2004)

[32] A. Kay, Perfect state transfer: Beyond nearest-neighbor couplings, Phys. Rev. A **73**, 032306 (2006)

[33] M. Reed and B. Simon, Methods of Modern Mathematical Physics, Vol. 1, Academic Press; 1st edition (1981)

[34] N. Hansen and S. Kern Evaluating the CMA Evolution Strategy on Multimodal Test Functions. In: Eighth International Conference on Parallel Problem Solving from Nature PPSN VIII, Proceedings, pp. 282-291, Berlin, Springer-Verlag (2004)

[35] M. Schmidt am Busch, F. Muh, M. E. Madjet and T. Renger, The eighth bacteriochlorophyll completes the excitation energy funnel in the FMO protein, J. Phys. Chem. Lett. **2**, 93-98 (2011)

[36] P. Huo and D. F. Coker, Theoretical study of coherent excitation energy transfer in cryptophyte Phycocyanin 645 at Physiological Temperature, J. Phys. Chem. Lett. **2**, 825-833 (2011)

[37] J. Sperling, A. Nemeth, J. Hauer, D. Abramavicius, S. Mukamel, H. F. Kauffmann and F. Milota, Excitons and Disorder in Molecular Nanotubes: A 2D Electronic Spectroscopy Study and First Comparison to a Microscopic Model, J. Phys. Chem. A **114**, 8179-8189 (2010)

[38] J. P. Bothma, J. B. Gilmore and R.H. McKenzie, The role of quantum effects in proton transfer reaction in enzymes: quantum tunneling in a noisy environment? New. J. Phys. **12**, 055002 (2010)